

NASA TECHNICAL NOTE



NASA TN D-5011

C.1

NASA TN D-5011



LOAN COPY: RETURN TO
AFWL (WLIL-2)
KIRTLAND AFB, N MEX

TWO-BURN ESCAPE MANEUVERS WITH AN INTERMEDIATE COASTING ELLIPSE

by Edward A. Willis, Jr.

*Lewis Research Center
Cleveland, Ohio*



TWO-BURN ESCAPE MANEUVERS WITH AN
INTERMEDIATE COASTING ELLIPSE

By Edward A. Willis, Jr.

Lewis Research Center
Cleveland, Ohio

NATIONAL AERONAUTICS AND SPACE ADMINISTRATION

For sale by the Clearinghouse for Federal Scientific and Technical Information
Springfield, Virginia 22151 - CFSTI price \$3.00

ABSTRACT

Escape maneuvers having two burns separated by a coasting ellipse are compared with conventional single-burn maneuvers for low circular initial orbits and a wide range of launch energies. One- and two-stage vehicles with nuclear and chemical propulsion are considered. This two-burn escape mode yields significantly lower initial mass and engine size, and improved launch window capability.

TWO-BURN ESCAPE MANEUVERS WITH AN INTERMEDIATE COASTING ELLIPSE

by Edward A. Willis, Jr.

Lewis Research Center

SUMMARY

This report deals with a class of efficient trajectories for escaping from a circular geocentric parking orbit. Each trajectory consists of two distinct burns separated by coasting around an intermediate ellipse. Engines are assumed to operate with constant tangential thrust and constant jet velocity; initial mass is minimized by finding optimum initial accelerations and optimum startup, cutoff, relight, and staging points.

The initial masses, desirable engine sizes, burn times, and other main features of these trajectories are compared with those resulting from conventional single-burn maneuvers. For one- and two-stage vehicles with representative chemical and nuclear propulsion systems, the present maneuvers lead to initial mass savings ranging from a few percent at low launch energies to 25 percent or more for high energy missions. Mission durations are extended by a few hours or days which is insignificant compared to typical mission times.

The optimum maximum engine sizes (e. g. , the first-stage engine on a two-stage vehicle) are reduced about 40 percent. For one-stage vehicles, the total burn time is increased by a like amount; for two-stage vehicles, however, the maximum burn times (which occur in the top stage) are actually reduced. Nuclear engine burn times are generally under 1 hour.

Launch window ΔV penalties may be significantly reduced by taking advantage of economical plane-change maneuvers consisting of a small transverse thrust at apogee of the intermediate ellipse.

INTRODUCTION

Earth escape is the first and often the most difficult maneuver of an interplanetary mission. A conventional escape maneuver, illustrated in figure 1, consists of a single powered arc (arc a-b) leading from an initial circular parking orbit to the desired escape hyperbola. While these single-burn maneuvers are adequate for present needs, a con-

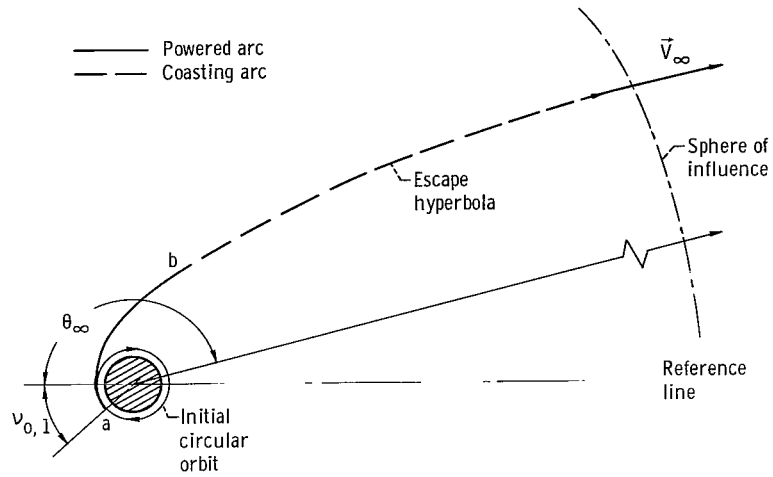


Figure 1. - Geometry of single-burn planetary escape maneuvers.

tinuing search for more efficient techniques is justified on the grounds that (1) the potential initial mass savings are likely to be more significant for future missions involving large payloads and/or high launch energies than they would be for current programs and (2) an improved escape maneuver technique, once developed, could be applied to probes as well as round-trip interplanetary missions.

This report deals with the performance characteristics and other features of the two-burn escape maneuver illustrated in figure 2. The first burn (arc a-b) leads from the initial orbit to an intermediate coasting ellipse. After coasting around the ellipse, the second burn (arc c-d) commences near perigee at a true anomaly $\nu_{0,2}$ and terminates in the desired escape hyperbola. (For present purposes, arcs a-b and c-d are each

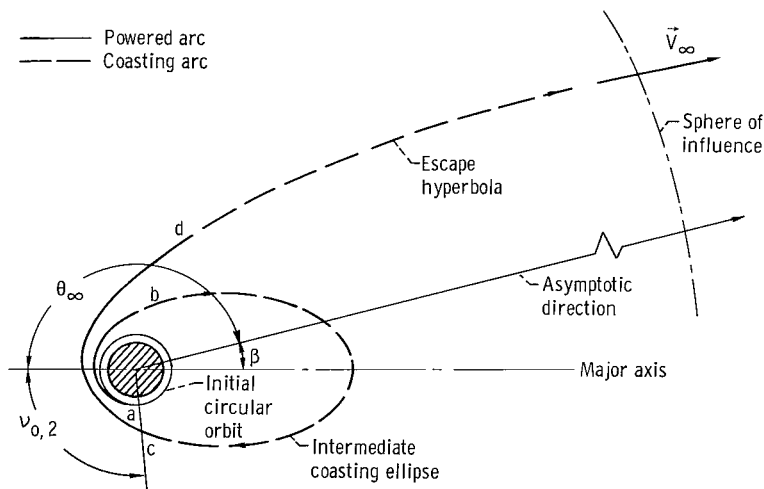


Figure 2. - Geometry of two-burn planetary escape maneuver.

treated as a single thrusting period even though staging may occur during one of these periods.)

This mode of escape is clearly a special case of the multiburn, "perigee-propulsion" trajectories studied in reference 1. That analysis, however, was primarily concerned with four- to twenty-burn maneuvers; and in a preliminary step, it actually implied that two-burn maneuvers were inferior to conventional ones (see fig. 3 of ref. 1). This report more realistically evaluates the merits of the less complicated, two-burn escape trajectory. In addition, it considers two-stage as well as one-stage vehicles, chemical as well as nuclear engines, and an inclusive range of launch energies.

These maneuvers are analyzed and discussed in terms of their effects on the following:

- (1) Initial mass, maneuver times, and other mission characteristics
- (2) Propulsion system parameters such as optimum acceleration levels, engine sizes, and burning times
- (3) Launch window ΔV penalties

ANALYSIS

The problem studied herein, as illustrated by figure 1, is to find trajectories for escaping from a given geocentric orbit with minimum initial mass. The conventional solution involves a single-burn maneuver as shown in figure 1 and has been extensively studied (ref. 2). The present analysis will develop methods for computing and optimizing the performance of two-burn maneuvers (shown in fig. 2) which involve coasting around an intermediate elliptic orbit.

Assumptions and Input Data

The following simplifying assumptions are used herein:

(1) Trajectories are planar, except in the "Launch window" sections, and are governed by an inverse-square gravitational field.

(2) Trajectory boundary conditions are defined by the initial parking orbit (assumed to be circular) and by the hyperbolic velocity vector \vec{V}_∞ at the sphere of influence. The latter is specified by prior interplanetary trajectory calculations such as those in references 3 and 4.

(3) The propulsion system operates with constant specific impulse and constant thrust. It is assumed that the desired \vec{V}_∞ direction is attained by an appropriate choice of the initial startup point (point a in fig. 1). The optimum pitch steering program is then

well approximated by tangential thrust. (See appendix of ref. 2.)

(4) Initial mass is computed on the basis of a simple linear scaling law (as opposed to detailed design studies). The same scaling constants are used for single-burn and two-burn maneuvers. Thus, possible effects of two-burn maneuvers on the weight or complexity of individual vehicle systems are neglected. It is assumed that penalties (which may result from the need for engine restart, longer coasting time, etc.) can be kept small by proper system design, and they are not accounted for in the results.

Methods of Computation

The specific equations used here are derived or attributed to references in this section. Symbols are defined in appendix A.

Initial mass growth. - Consider first a single-stage vehicle. If the burnout mass and trajectory boundary conditions are known, the initial mass is given by the following expression:

$$M_{O, 1} = \frac{M_{bo, 1}}{1 - k_{p, 1}} \quad (1)$$

where the propellant fraction $k_{p, 1}$ may be defined by numerically integrating the trajectory or by the classical rocket equation

$$k_{p, 1} = 1 - \exp \frac{\Delta V_1}{g_{\oplus, s} I_1} \quad (2)$$

A more useful form of equation (1) may be derived by dividing the burnout mass $M_{bo, 1}$ into hardware components which are known or can be estimated beforehand. These are defined as payload mass and additional increments proportional to propellant mass, thrust, and maximum acceleration. The resultant equation is

$$M_{bo, 1} = M_{pay, 1} + M_{ps, 1} + M_{fs, 1} + M_{as, 1} \quad (3)$$

In equation (3), $M_{pay, 1}$ is given; and it is assumed that the other three terms are respectively proportional to the propellant mass $M_{p, 1}$, the engine thrust F_1 , and the maximum acceleration loading $a_{max} M_{pay, 1}$ imposed by the payload. That is,

$$M_{ps, 1} = k_{ps, 1} M_{p, 1} = k_{ps, 1} k_{p, 1} M_{o, 1} \quad (4)$$

$$M_{fs, 1} = \frac{k_{fs, 1} F_1}{g_{\oplus, s}} = k_{fs, 1} a_{o, 1} M_{o, 1} \quad (5)$$

$$M_{as, 1} = k_{as, 1} M_{pay, 1} a_{max, 1} = \frac{k_{as, 1} M_{pay, 1} a_{o, 1}}{1 - k_{p, 1}} \quad (6)$$

where the initial acceleration parameter a_o is measured in units of the Earth's surface gravity. Substituting equations (4) to (6) into equation (3) and the result into equation (1) yields the scaling law

$$M_{o, 1} = h_1 M_{pay, 1} \quad (7a)$$

where h_1 , the first stage initial mass parameter, is

$$h_1 = \frac{1 + k_{as, 1} a_{o, 1} (1 - k_{p, 1})^{-1}}{1 - k_{p, 1} (1 + k_{ps, 1})^{-1} a_{o, 1}^{k_{fs, 1}}} \quad (7b)$$

There is, of course, an analogous formula for the second stage of a two-stage vehicle. In this case, the payload of stage one is the initial mass of stage two; hence,

$$M_{o, 1} = h_1 h_2 M_{pay, 2} \quad (7c)$$

Values of the inert mass fractions k_{ps} , k_{fs} , k_{as} , and specific impulse I used herein are listed in table I for representative chemical and nuclear propulsion systems. The numbers in table I are representative of each type of propulsion system, but do not correspond to specific hardware.

Since the apogee is generally above 10 Earth radii, the ascending and descending sides of the coasting ellipse each penetrate the Van Allen radiation belts in much the same manner as the subsequent escape hyperbola. The consequently increased exposure to radiation flux may be reflected in larger doses or heavier shielding requirements (i. e., higher M_{pay}) for manned mission. The size and seriousness of this effect can only be assessed in terms of a specific mission and shield design. In one study (ref. 5), for example, it was found that the Van Allen dose per penetration is only a few rem out

TABLE I. - STAGE AND PROPULSION SYSTEM INPUT PARAMETERS

Type	Specific impulse, I, sec	Thrust-sensitive weight fraction, k_{fs}^a	Propellant-sensitive weight fraction, k_{ps}^b	Acceleration-sensitive weight fraction, k_{as}^c
Solid-core nuclear	800	^d 0.30	^e 0.25	0.025
Chemical (LOX-LH ₂)	425	.06	.09	.025

^a $k_{fs} \triangleq M_{fs}/F$; includes engine, thrust structure, feed ducts, plumbing, actuators, and controls.

^b $k_{ps} \triangleq M_{ps}/p$; includes tank, gas and liquid residuals, insulation, and pressurization system.

^c $k_{as} \triangleq M_{as}/a_{max} M_{pay}$; primarily interstage structure.

^d Also includes propellant radiation shielding.

of round-trip totals approximating 100 rem; in such cases, the two additional penetrations are not likely to be a major factor.

Burn times. - A parameter of special interest for nuclear engine development is the maximum burn time $T_{bo, max}$. For a first stage, $T_{bo, 1}$ is given by

$$T_{bo, 1} = \frac{I_1 k_{p, 1}}{a_{o, 1}} \quad (8)$$

and there is a similar formula for $T_{bo, 2}$ if a two-stage vehicle is used. The maximum value is then

$$T_{bo, max} = \begin{cases} T_{bo, 1} & \text{single stage} \\ \text{Max}(T_{bo, 1}, T_{bo, 2}) & \text{two stage} \end{cases} \quad (9)$$

Trajectory equations. - The trajectories for single-burn maneuvers and for each individual burn of a two-burn maneuver may be computed just as they were in reference 2. It only remains to match the two segments of a two-burn maneuver and minimize the consequent values of $M_{o, 1}$.

The appropriate matching conditions are simply that

$$V_{\infty, bo, 1}^2 = V_{\infty, co}^2 = V_{\infty, o, 2}^2 \quad (10)$$

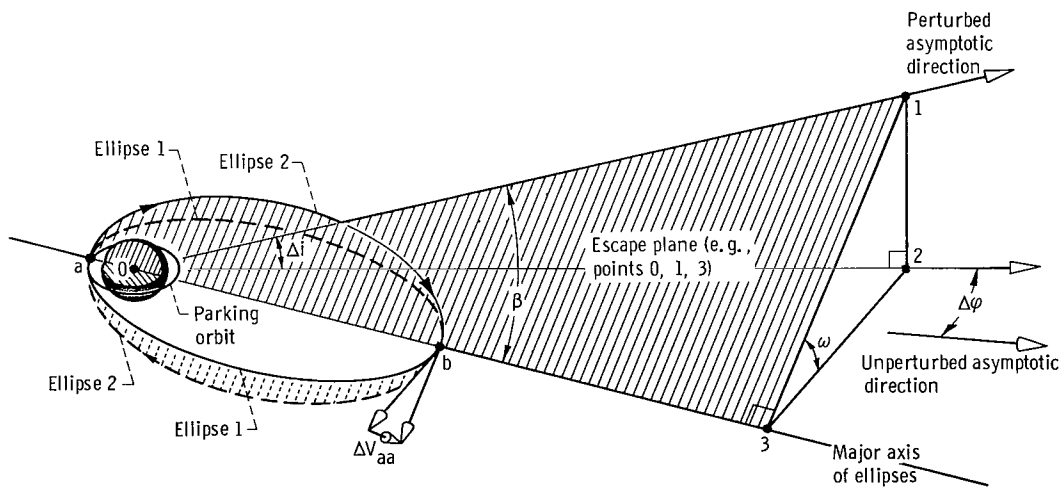
and (for single-stage vehicles only)

$$k_{p, o, 2} = k_{p, bo, 1} \quad (11)$$

The first condition merely expresses conservation of energy along the coasting ellipse, and the second indicates that a partially spent stage is being relit.

The trajectory computer code of reference 2 was extended to include the initial mass equations (eqs. (7)) and matching equations (10) and (11). A numerical optimization routine was adapted from reference 6 to directly minimize $M_{O, 1}$ in terms of the search variables, $a_{O, 1}$, $a_{O, 2}$, $V_{\infty, sp}^2$, $V_{\infty, co}^2$, and $\nu_{O, 2}$.

Launch window ΔV penalties. - If there is an unexpected delay after the original parking orbit is established, the nominal boundary conditions may be perturbed (e. g., by orbital precession) as indicated in figure 3. Here, the original orbit and nominal asymptotic direction lie in the plane of the paper; relative to this, the new asymptotic direction is perturbed by an in-plane component $\Delta\phi$ and an out-of-plane component Δi .



CD-10099-30

Figure 3. - Geometry of apogee-plane-change (APC) maneuver.
(Original parking orbit in plane of paper (e. g., points 0, 2, 3).)

The in-plane perturbation $\Delta\varphi$ need not cause a ΔV penalty as long as it is possible to choose an appropriate power-on point. The out-of-plane component, however, requires a plane-change maneuver to be accomplished prior to or during the escape maneuver. For the present two-burn maneuvers, it is possible to accomplish the plane change very economically by firing transversely at the apogee of the intermediate ellipse. That is, the first burn (point a) yields an ellipse which is still in the original plane (the plane of the paper, points 0, 2, 3). At apogee, a transverse impulse ΔV_{lwp} is applied to rotate the ellipse through an angle ω , resulting in ellipse 2. The rotation angle ω is chosen so that ellipse 2 lies in the "escape plane" (points 0, 1, 3) defined by the perturbed asymptotic direction and the common major axis of the ellipses. Angle ω and the power-on point $\nu_{0,2}$ on ellipse 2 can usually be oriented for an optimum angle escape maneuver in the escape plane (i. e., the asymptotic central angle of the final escape trajectory, measured from the semimajor axis, can be chosen on the basis of minimum ΔV).

If $\theta_{\infty, opt}$ denotes this optimum asymptotic central angle for escaping from an ellipse (numerical values are given in ref. 2), the angle β (3, 0, 1) must satisfy the following condition:

$$\beta = 180^\circ - \theta_{\infty, opt}$$

Since angles (0, 2, 1), (0, 3, 1), and (1, 2, 3) are right angles, it follows that ω and $\theta_{\infty, opt}$ are related by

$$\sin \omega = \frac{\sin \Delta i}{\sin(180^\circ - \theta_{\infty, opt})} = \frac{\sin \Delta i}{\sin \theta_{\infty, opt}} \quad (12a)$$

Then ΔV_{lwp} is given by

$$\Delta V_{lwp} = 2V_{aa} \sin \frac{\omega}{2} \quad (12b)$$

In order for the preceding steps to be feasible, equations (12) imply that

$$\Delta i \leq (180^\circ - \theta_{\infty, opt}) \quad (13)$$

If equation (13) is not satisfied, it would still be possible (for instance) to use an ω of 90° and a directionally constrained pitch steering program of the type discussed in refer-

ence 7; the directional constraint requires that

$$\theta_{\infty, \text{act}} = 180^\circ - \Delta i \quad (14)$$

These results, which pertain to the present two-burn escape mode, will be compared later with the yaw steering and "dog-leg" alternatives that apply to conventional maneuvers.

A third type of perturbation, in the magnitude of \vec{V}_∞ , can also occur. Its effects are unavoidable but are approximately the same for one- and two-burn maneuvers. The effect of V_∞ itself¹ will be discussed parametrically in later sections.

RESULTS AND DISCUSSION

This section will proceed by first illustrating how the previously described calculations are applied to one- and two-burn maneuvers with one- and two-stage vehicles. Numerical comparisons between the one- and two-burn results are then presented; these are further illustrated by specific examples. Finally, some secondary features of the two-burn maneuvers are briefly discussed.

Optimum One- and Two-Burn Maneuvers

Single-stage vehicles. - Under the assumptions presented in the ANALYSIS section, the initial acceleration $a_{o, 1}$ is the only parameter available for optimization in the case of a single-burn, single-stage vehicle. In this case, $M_{o, 1}$ is minimized by balancing propellant mass (which increases as $a_{o, 1}$ decreases) against engine system mass (which is proportional to $a_{o, 1}$). This illustrated by the upper (dash-dotted) curve in figure 4 for a high-energy ($v_\infty^2 = V_\infty^2/V_c^2 = 2$) single-burn maneuver using a single nuclear engine stage. In this case, the minimum value of $h_1 = M_{o, 1}/M_{\text{pay}, 1} \approx 9.3$ occurs for $a_{o, 1} \approx 0.21$. The entire curve, however, lies significantly above the theoretical (and physically unattainable) dashed curve derived by neglecting all gravity losses.

For the two-burn maneuvers, it is possible to optimize the energy of the intermediate ellipse ($v_{\infty, c0}^2$) and the location of the second-burn startup point ($v_{o, 2}$) as well as

¹Note that the symbol V_∞ indicates the magnitude $|\vec{V}_\infty|$, of the asymptotic velocity vector.

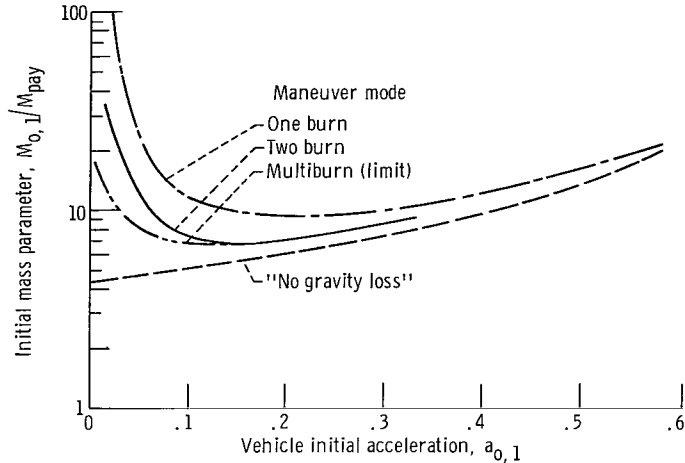


Figure 4. - Optimization of initial acceleration. Single-stage vehicles; nuclear stage inputs from table I; launch energy parameter $v_{\infty,co}^2 = 2$; initial orbit radius, $1.1 R_{\oplus}$.

$a_{O,1}$. The effects of ellipse energy² and startup point³ are discussed in reference 2 and not illustrated here. In brief, optimizing $v_{\infty,co}^2$ involves trading between first- and second-burn gravity losses; optimizing $\nu_{O,2}$ minimizes the second-burn gravity loss (for given $v_{\infty,co}^2$) by placing as much of it as possible in the high-velocity region near perigee.

The solid curve in figure 4 illustrates the effect of $a_{O,1}$ on two-burn maneuvers with $\nu_{O,2}$ and $v_{\infty,co}^2$ optimized at every point. There is a clear reduction in $M_{O,1}/M_{pay,1}$ (6.9 against 9.3) in comparison with the single-burn result. The corresponding value of $a_{O,1,opt}$ is reduced from 0.21 to 0.15 $g_{\oplus,s}$. Thus, the initial mass saving is attributable to reductions in both propellant- and thrust-sensitive masses, $M_p + M_{ps}$ and M_{fs} .

Comparison with multiburn maneuvers. - In order to determine whether still greater savings could be made by using more than two burns, the N-burn analysis of reference 1 was carried to the limit of very large N. In the limit, the first N-1 burns approach small impulses at perigee of successive ellipses and suffer negligible gravity losses. The N-1th ellipse is very nearly parabolic; the Nth and final burn must then supply the remaining energy increment between $v_{\infty}^2 \approx 0$ and the desired launch energy. Once the condition $v_{\infty}^2 = 0$ has been passed, it is no longer possible to coast back into the perigee re-

²See fig. 13 and pp. 50-51 of ref. 2. The present ellipse energy $v_{\infty,co}^2$ is related to the orbital eccentricity e_{po} used in ref. 2 by the formula $v_{\infty,co}^2 = e_{po}^2 - 1$.

³See fig. 12 and pp. 49-50 of ref. 2. The present $\nu_{O,2}$ is labeled ν_{po} in ref. 2.

gion. Thus, while negligible in the first $N-1$ burns, gravity losses are unavoidable in the N^{th} and final burn.

The performance resulting from this idealized multiburn limit is indicated by the remaining curve in figure 4. The performance margin thus obtained is clearly insignificant when two- and N -burn results are compared on the basis of optimum values of $a_{o,1}$. In the present example, the two-burn approach yields over 98 percent of the ultimate $M_{o,1}$ saving and about 87 percent of the ultimate reduction in $a_{o,1,opt}$. Hence, it is concluded that the multiburn technique ($N > 2$) is of interest primarily when $a_{o,1}$ is limited a priori to below optimum values such as 0.01 to 0.05 $g_{\oplus,s}$ (the range considered in ref. 1).

Two-stage vehicles. - For a two-stage vehicle using conventional maneuvers, the initial accelerations $a_{o,1}$ and $a_{o,2}$ and the staging-point energy $v_{\infty,sp}^2$ can all be chosen for minimum initial mass. With two-burn maneuvers, the parameters $v_{\infty,co}^2$ and $\nu_{o,2}$ are also available. Note that staging may occur either during the elliptic coast or at an optimum point during the second burn. Thus, the thrust history during the second burn may either be continuous, or it may be consecutive with a step change in thrust and acceleration at the staging point, depending upon where the optimum point occurs.

The effects of a_o , $v_{\infty,co}^2$, and $\nu_{o,2}$ were discussed previously for the single-stage case and have similar effects when two stages are considered. Figure 5 shows the effect of $v_{\infty,sp}^2$ (for optimum a_o 's, $v_{\infty,co}^2$, and $\nu_{o,2}$) again for high-energy maneuvers with $v_{\infty}^2 = 2$. For single-burn (consecutive thrust) maneuvers, the dash-dotted curve, the minimum of $M_{o,1}/M_{pay}$ is 6.3 and occurs at $v_{\infty,sp}^2 \approx 0.55$. (The minimums are de-

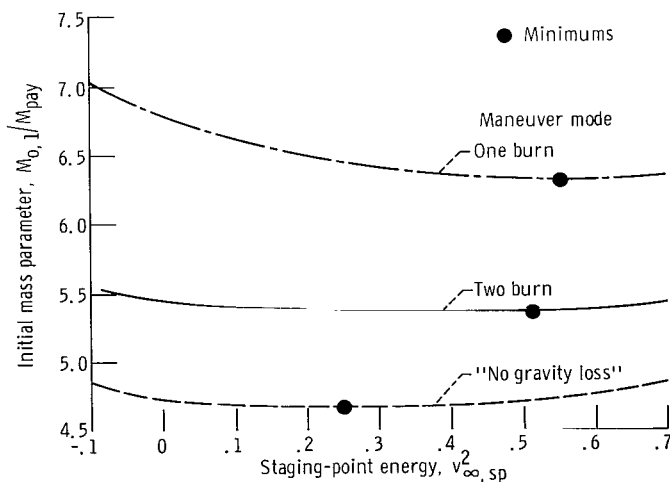


Figure 5. - Optimization of staging-point energy. Two-stage vehicles; nuclear stage inputs from table I; launch energy parameter $v_{\infty}^2 = 2$.

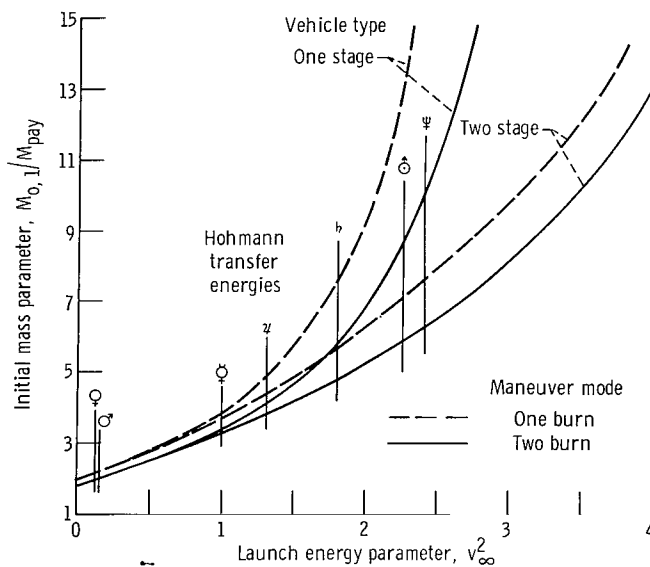
noted by solid circles and were determined analytically.) As in the previous case, the two-burn maneuver (solid curve) yields a substantial performance gain and more closely approaches the unattainable limit where there are no gravity losses. The two-burn minimum is also remarkably flat, and a later section will indicate how this fact can be used to advantage.

Comparison of One- and Two-Burn Maneuvers

Having now illustrated the considerations involved in optimizing the present two-burn trajectories, it remains to compare their initial masses, maneuver times, and engine sizes with those resulting from single-burn maneuvers over a range of launch energies.

Initial mass parameters. - The dimensionless initial mass $M_{o,1}/M_{pay,1}$ is plotted against the dimensionless launch energy parameter ($v_{\infty}^2 = V_{\infty}^2/V_c^2$) for one- and two-stage vehicles with nuclear propulsion, and for one- and two-burn maneuvers in figure 6(a). (The vertical lines below the planet symbols indicate the respective Hohmann trip Earth-launch energies in these dimensionless units. These are, of course, minimum values; "fast" trips can easily require as much as one v_{∞}^2 unit more energy in each case.)

Trajectory details for the cases covered by figure 6(a) are listed in table II for each of the four trajectory-vehicle combinations studied. Consider first the single-stage-



(a) Nuclear stages.

Figure 6. - Effect of launch energy parameter. One- and two-stage vehicles; nuclear stage inputs from table I; optimum initial acceleration a_0 and staging-point energy $v_{\infty, sp}^2$.

TABLE II. - SUMMARY OF ESCAPE MANEUVER CHARACTERISTIC (NUCLEAR STAGES)^a

(a) Single stage, single burn

Launch energy parameter, v_{∞}^2 , dimensionless (b)	Minimum initial mass parameter, $M_{O, 1}/M_{pay}$	Optimum initial acceleration, a_o , Earth gravity	Propulsive velocity increment, Δv_1 , dimensionless (b)	Impulsive velocity increment, Δv_{imp} , dimensionless (b, c)	Hyperbolic excess speed	
					v_{∞} , dimensionless (b, c)	V_{∞} , km/sec (c)
-0.1000	1.82	0.134	0.405	0.378	-----	-----
.0625	2.02	.148	.470	.436	0.250	1.89
.2500	2.28	.156	.545	.500	.500	3.88
.5000	2.71	.177	.634	.581	.707	5.34
1.0000	3.85	.196	.808	.732	1.000	7.55
1.5000	5.75	.208	.969	.871	1.223	9.24
2.0000	9.34	.208	1.124	1.000	1.414	10.68
2.5000	-----	-----	-----	1.121	1.580	11.93
3.0000	-----	-----	-----	1.235	1.732	13.09
4.0000	-----	-----	-----	1.450	2.000	15.10

(b) Single stage, two burn

Launch energy parameter, v_{∞}^2 , dimensionless (b)	Minimum initial mass parameter, $M_{O, 1}/M_{pay}$	Optimum initial acceleration, a_o , Earth gravity	Parameters of coasting ellipse			Propulsive velocity increment, dimensionless	
			Energy, $v_{\infty, co}^2$ (b)	Period, T_{co} , hr	Optimum initial true anomaly, ν_{co} , deg	Burn 1 (b)	Burn 2 (b)
0.0625	1.92	0.097	-0.568	3.9	47.2	0.202	0.254
.2500	2.14	.110	-.508	4.6	47.5	.228	.296
.5000	2.49	.118	-.450	5.5	56.1	.254	.361
1.0000	3.39	.135	-.343	8.3	61.6	.298	.482
1.5000	4.74	.152	-.199	19	51.4	.358	.570
2.0000	6.93	.156	-.106	48	53.8	.396	.676
2.5000	11.20	.156	-.086	66	57.5	.405	.806

^aInputs from table I.

^bVelocities are in units of Earth circular speed at $R_{po} = 1.1 R_{\oplus}$, that is, 7.55 km/sec.

^cThese values also apply to table II(b) to (d) and table III.

TABLE II. - Concluded. SUMMARY OF ESCAPE MANEUVER CHARACTERISTICS (NUCLEAR STAGES)

(c) Two stage, single burn

Launch energy parameter, v_{∞}^2 , dimensionless (b)	Minimum initial mass parameter, $M_{O, 1}/M_{pay}$	Optimum initial acceleration, a_O , Earth gravity		Optimum staging-point energy, $v_{\infty, sp}^2$ (b)	Propulsive velocity increments, Δv	
		Stage 1	Stage 2		Stage 1 (b)	Stage 2 (b)
		1.0000	3.63		0.199	0.103
1.5000	4.75	.211	.109	.388	.579	.425
2.0000	6.23	.217	.106	.549	.637	.524
3.0000	9.97	.221	.081	.858	.747	.704
4.0000	15.95	.219	.058	1.140	.844	.863

(d) Two stage, two burn

Launch energy parameter, v_{∞}^2 , dimensionless (b)	Minimum initial mass parameter, $M_{O, 1}/M_{pay}$	Optimum initial acceleration, a_O , Earth gravity		Optimum staging-point energy, $v_{\infty, sp}^2$ (b, d)	Parameters of coasting ellipse			Propulsive velocity increments, Δv	
		Stage 1	Stage 2		Energy, $v_{\infty, co}^2$ (b)	Period, T_{co} , hr	Optimum initial true anomaly, ν_{co} , deg	Stage 1 (b)	Stage 2 (b)
		Optimum $v_{\infty, sp}^2$							
1.0000	3.28	0.149	0.119	-0.106	-0.106	48	-64.0	0.398	0.396
1.5000	4.20	.151	.160	.417	-.081	72	-58.9	.451	.489
2.0000	5.37	.158	.144	.511	-.135	33	-52.4	.618	.486
3.0000	8.54	.154	.097	.985	-.214	17	-53.1	.767	.631
4.0000	13.35	.149	.058	1.29	-.199	18	-57.3	.867	.796
Early abort capability, $d \ v_{\infty, sp}^2 \leq 0$									
1.5000	4.22	0.161	0.139	-0.02	-0.02	592	-64.4	0.430	0.519
2.0000	5.46	.165	.156	-.02	-.02	592	-65.7	.430	.665
3.0000	9.63	.172	.172	-.02	-.02	592	-70.8	.430	.941

^bVelocities are in units of Earth circular speed at $R_{po} = 1.1 R_{\oplus}$, that is, 7.55 km/sec.

^dFor the last three cases, it is assumed that $v_{\infty, sp}^2 = v_{\infty, co}^2 \leq -0.02$ in order to maintain early abort capability through second-stage ignition.

TABLE III. - SUMMARY OF ESCAPE MANEUVER CHARACTERISTICS, CHEMICAL STAGES^a

(a) Single stage, single burn

Launch energy parameter, v_{∞}^2 , dimensionless (b)	Minimum initial mass parameter, $M_{O,1}/M_{pay}$	Optimum initial acceleration, a_o , Earth gravity	Propulsive velocity increment, ΔV_1 (b)
-0.1000	2.35	0.253	0.385
.0625	2.70	.277	.444
.2500	3.17	.302	.510
.5000	3.91	.303	.594
1.0000	6.04	.328	.751
1.5000	9.85	.352	.898
2.0000	17.92	.352	1.035

(b) Single stage, two burn

Launch energy parameter, v_{∞}^2 , dimensionless (b)	Minimum initial mass parameter, $M_{O,1}/M_{pay}$	Optimum initial acceleration, a_o , Earth gravity	Parameters of coasting ellipse			Propulsive velocity increment, Δv	
			Energy, $v_{\infty,co}^2$	Period, T_{co} , hr	Optimum initial true anomaly, ν_{co} , deg	Burn 1	Burn 2
						(b)	(b)
0.0625	2.35	0.156	-0.579	----	-27.5	0.194	0.248
.2500	2.70	.197	-.535	----	-23.6	.212	.294
.5000	3.17	.197	-.499	----	-28.6	.231	.358
1.0000	5.63	.197	-.395	----	-34.3	.270	.476
1.5000	8.85	.205	-.307	----	-36.7	.306	.585
2.0000	14.97	.213	-.228	15.3	-37.1	.337	.687

^aInputs from table I.

^bVelocities are in units of Earth circular speed at $R_{po} = 1.1 R_{\odot}$, that is, 7.55 km/sec.

vehicle results (the two upper curves). The two-burn mode evidently yields a lower mass parameter for all launch energies; the margin increases from around 5 percent at low energies ($v_{\infty}^2 < 0.25$) up to a conspicuous 25 percent or more for high-energy missions ($v_{\infty}^2 > 2.0$). As might be expected, two-stage vehicles (the two lower curves) yield generally lower values of $M_{O,1}/M_{pay}$. But in this case again, the two-burn mode yields 5 to 20 percent savings. Another point of interest is that the single-stage, two-burn combination gives lower values of $M_{O,1}/M_{pay}$ than the two-stage, single-burn option out to moderately high energies (e.g., $v_{\infty}^2 \approx 1.5$). These two alternatives may be compared on the basis of more nearly equal complexity.

Similar comparisons are made for chemical vehicles in table III and figure 6(b).

TABLE III. - Concluded. SUMMARY OF ESCAPE MANEUVER
CHARACTERISTICS, CHEMICAL STAGES

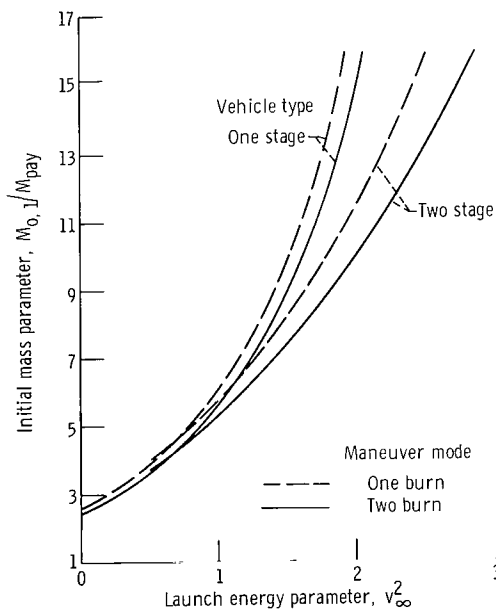
(c) Two stage, single-burn

Launch energy parameter, v_{∞}^2 , dimensionless (b)	Minimum initial mass parameter, $M_{o,1}/M_{pay}$	Optimum initial acceleration, a_o , Earth gravity		Optimum staging-point $v_{\infty, sp}^2$ (b)	Propulsive velocity increments, Δv	
		Stage 1	Stage 2		Stage 1 (b)	Stage 2 (b)
		0.5000	4.03		0.368	0.344
1.000	5.80	.418	.394	-.031	.406	.349
1.5000	8.20	.452	.423	.173	.478	.423
2.000	11.48	.478	.454	.369	.544	.493

(d) Two stage, two burn

Launch energy parameter, v_{∞}^2 , dimensionless (b)	Minimum initial mass parameter, $M_{o,1}/M_{pay}$	Optimum initial acceleration, a_o , Earth gravity		Parameters of coasting ellipse			Propulsive velocity increments, Δv	
		Stage 1	Stage 2	Energy, $v_{\infty, co}^2$ (b)	Period, T_{co} , hr	Optimum initial true anomaly, ν_o , deg	Stage 1	Stage 2
							(b)	(b)
0.5000	3.73	0.235	0.219	-0.335	8.6	-31.8	0.293	0.207
1.0000	5.30	.280	.262	-.138	31.7	-35.0	.369	.378
1.5000	7.37	.306	.297	-.020	59.2	-36.5	.412	.477
2.0000	10.28	.315	.327	-.020	59.2	-38.8	.412	.610

^bVelocities are in units of Earth circular speed at $R_{po} = 1.1 R_{\oplus}$, that is, 7.55 km/sec.



(b) Chemical stages.

Figure 6. - Concluded.

Clearly, the previously mentioned trends hold also in this case; however, the percentage improvements are smaller because of the generally lower inert mass fraction applicable to chemical systems.

Under the assumptions of the present analysis, the two-burn escape mode yields lower mass fractions than the conventional single-burn maneuver at all launch energies for one- and two-stage vehicles and for nuclear and chemical propulsion. The reduction is largest for nuclear propulsion and for large launch energies; it increases from about 5 percent for typical (420 to 540 days) Mars or Venus round trips up to 20 or 25 percent for trips to Jupiter and beyond.

Maneuver times. - For the two-burn mode, the maneuver time (from first-burn startup to second-burn cutoff) will clearly be extended by an amount ΔT_m which is approximately equal to the period of the coasting ellipse. This must be counted as a mission time penalty if maneuvers are compared on the basis of identical \vec{V}_∞ 's (and hence, identical injection dates). The time penalty ΔT_m is plotted against the launch energy parameter in figure 7 for one- and two-stage nuclear vehicles (the results for chemical

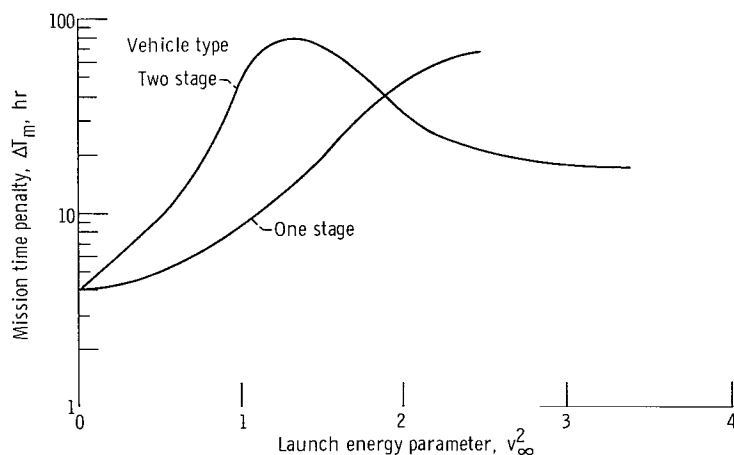


Figure 7. - Mission time penalties for two-burn maneuvers. Nuclear stages: inputs from table I; optimum initial acceleration a_0 and staging-point energy $v_{\infty, sp}^2$.

vehicles are similar and are not illustrated here). The values of ΔT_m range from 4 to 72 hours; this is, in most cases, a very small fraction of the total mission time.

The steady increase in ΔT_m for the one-stage vehicle results because, as the launch energy increases, the energy imparted by the first burn also increases. The energy and, hence, the period of the coasting ellipse, which is the mission time penalty, consequently increases. The peak evident in the two-stage curve comes about for the

following reasons. For $v_{\infty}^2 \leq 1$, the optimum values of $v_{\infty,co}^2$ and $v_{\infty,sp}^2$ are found to be the same. Thus, the ellipse energy (and hence, period) increases rapidly with v_{∞}^2 in order to maintain a roughly equal ΔV distribution between the two stages. At higher launch energies, this same tendency toward even ΔV distributions forces the staging point out into the second burn. The first stage then encompasses the first burn, the coast, and part of the second burn; it therefore resembles a single stage escaping to a lower value of v_{∞}^2 .

Engine sizes. - The benefits of the two-burn escape mode are by no means limited to initial mass savings. The accompanying decrease of $a_{o,opt}$ (recall fig. 4) implies that smaller, and presumably lighter and less costly, engines could be used. This is an especially important consideration for nuclear engines, and the present section is limited to that case.

For given values of k_{fs} , the engine size is proportional to its thrust, given by $a_o M_o g_{\oplus,s}$. Thus, engine size reductions depend equally upon decreasing M_o and a_o . Initial mass savings were illustrated in figure 6, and figure 8 now compares the values of

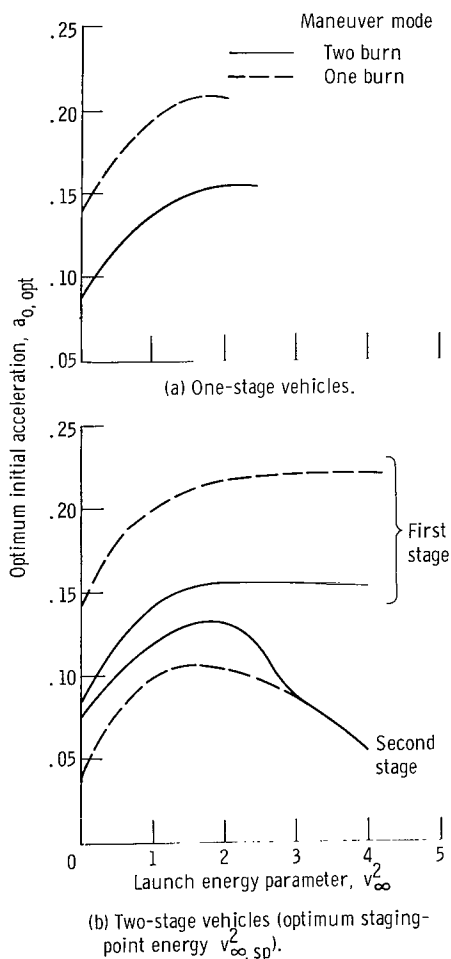


Figure 8. - Optimum initial accelerations for nuclear stages. Inputs from table 1.

$a_{o, \text{opt}}$ for conventional and two-burn maneuvers.

With single-stage vehicles (fig. 8(a)), both maneuvers yield similar trends in that $a_{o, \text{opt}}$ first increases as v_{∞}^2 increases, reaching a peak near $v_{\infty}^2 = 1.5$, and then remaining nearly constant. The two-burn values, however, are typically 30 percent below those for conventional maneuvers.

For two-stage vehicles (fig. 8(b)), $a_{o, \text{opt}}$ for the first stage increases toward a nearly constant value at high energies, just as it did in the single-stage case; $a_{o, 1}$ reductions of roughly 30 percent are also seen for the two-burn trajectory mode. The upper stages, however, display a different trend, that is, a very pronounced peak of $a_{o, 2, \text{opt}}$ at intermediate energies. For conventional maneuvers, the initial increase in $a_{o, 2}$ represents an effort to hold the powered trajectory in a relatively low-altitude, high-velocity regime. The gravity loss reductions thus obtained, however, are offset by progressively increasing engine masses at intermediate energies. At very large energies, moreover, the propellant fraction $k_{p, 2}$ will approach unity whether gravity losses are large or small. It is then clear from equation (7b) that the only remaining path to low mass is to decrease $a_{o, 2}$ again, which means to use a relatively small engine. The two-burn mode, as previously mentioned, tends to decrease the mean altitude of the second burn. Thus, the second burn optimizes at a higher value of $a_{o, 2}$ because it lies in a region of higher velocity and a stronger gravity field.

As pointed out previously, the actual reductions in engine size depend equally upon reductions of the initial mass and the initial acceleration. The combined effects of these variables may be seen clearly in the relative engine thrust parameter which is defined by

$$f = \frac{F}{M_{\text{pay}} g_{\oplus, s}} = h a_o$$

(a_o in units of $g_{\oplus, s}$) and is plotted against v_{∞}^2 in figure 9. (It should be understood that f is a relative thrust parameter. Therefore, figure 9 describes the effect of exchanging a one-burn for a two-burn Earth escape maneuver in a given mission. It does not necessarily indicate the effect of v_{∞}^2 on absolute engine size however, because the normalizing factor M_{pay} can include elements (such as a Mars capture stage) whose mass would tend to vary with v_{∞}^2 .) It is evident from these curves that for single-stage vehicles and for the first stage of a two-stage vehicle, the percentage engine size reduction is fairly constant at about 40 percent. (Equivalently, the number of engines in a cluster may be reduced by 40 percent.) This may be compared to $M_{o, 1}$ savings ranging from only a few percent at low energies to roughly 20 percent for $v_{\infty}^2 > 2$, and to $a_{o, 1}$ reductions decreasing from nearly 40 percent to roughly 20 percent over the same energy interval.

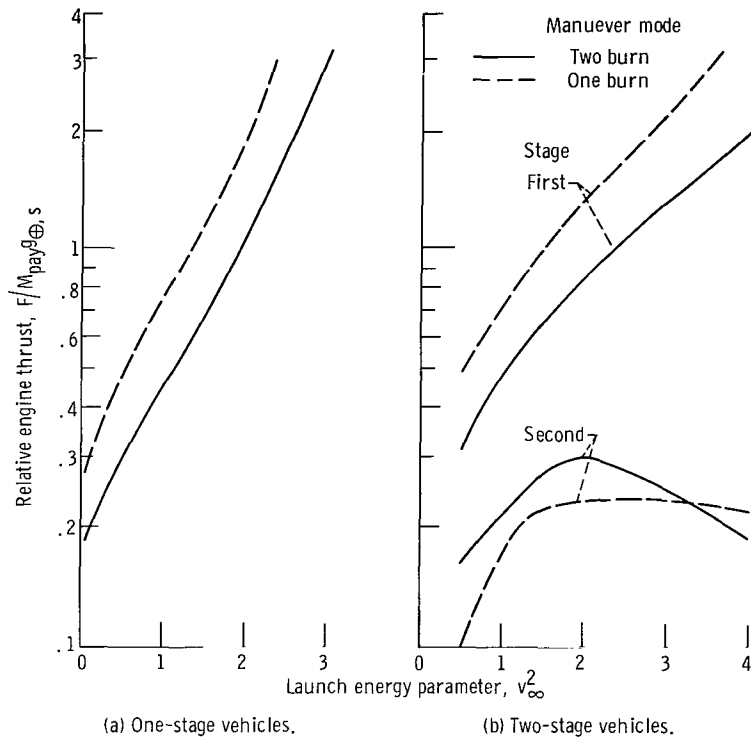


Figure 9. - Optimum thrust levels for nuclear stages. Inputs from table I.

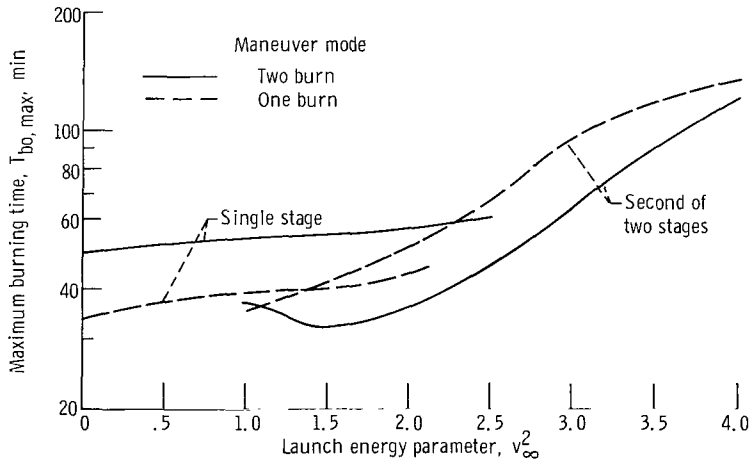


Figure 10. - Maximum required burning times for nuclear stages. Inputs from table I; optimum initial acceleration a_0 and staging-point energy $v_{\infty, sp}^2$.

On the other hand, the second stage of a two-stage vehicle will, except at the highest energies, require a larger engine rather than a smaller one when the two-burn mode is used. But by adding ordinates for the one-burn and two-burn cases (stage 1 and stage 2 values of f), it is clear that the two-burn approach always involves a smaller total powerplant weight (i. e., the first-stage decrease exceeds the second-stage increase).

Burn times. - As previously mentioned, the maximum burn time $T_{bo, max}$ is of great significance from the viewpoint of designing and developing a nuclear rocket engine reactor core. By referring again to equations (8) and (9), it will be recalled that $T_{bo, max}$ represents the total accumulated burn time on one stage (for a two-stage vehicle, the greater of the stage 1 and stage 2 values is used). Thus, $T_{bo, max}$ varies inversely with either $a_{o, 1}$ or $a_{o, 2}$ and will, therefore, show trends opposite to those illustrated by figures 8 and 9.

In figure 10, $T_{bo, max}$ is plotted against v_{∞}^2 for the same nuclear engine cases that were considered in the preceding section. For single-stage vehicles, the two-burn mode (upper solid curve) requires definitely longer burn times than the one-burn mode (dashed curve). Nevertheless, the actual values do not exceed 60 minutes, which is probably a reasonable design goal for a first-generation rocket reactor.

For two-stage vehicles, $T_{bo, max}$ is almost invariably associated with the upper stage. Therefore, just as $a_{o, 2}$ was seen to increase in the previous section, $T_{bo, max} = T_{bo, 2}$ now decreases when two-burn maneuvers are used. This has the practical effect that significantly higher launch energies can be achieved before burning time limitations become binding.

Utilization of nonoptimum engine sizes. - One method of providing powerplants for a wide variety of missions would be to approximate the thrust curves of figure 9 by clustering a discrete number of standard units. If this were done, the true optimum thrust ratios shown previously would seldom be achieved. The penalty for nonoptimum a_o was illustrated in figure 4 for a single-stage vehicle and a high launch energy. Referring again to that figure reveals that perturbations in a_o of ± 25 percent would not cause weight penalties greater than 5 percent for either trajectory mode. Thus, clusters typical comprising four or five engines can provide a rather close approach to the optimum sized results discussed elsewhere in this report.

Launch window ΔV 's. - The launch window problem may be resolved into three major components, that is, changes in (1) the magnitude of \vec{V}_{∞} , (2) the azimuthal direction of \vec{V}_{∞} , and (3) the inclination of \vec{V}_{∞} relative to the parking orbit plane. The effect of V_{∞} , shown in figure 6, is similar for one- and two-burn maneuvers. As previously mentioned, azimuthal changes need not cause any penalty at all if the proper power-on point is chosen. This leaves inclination changes as a major offender from the launch window viewpoint, and one that may be radically influenced by the escape mode used. The plane-changing ΔV penalties for one- and two-burn maneuvers are compared in

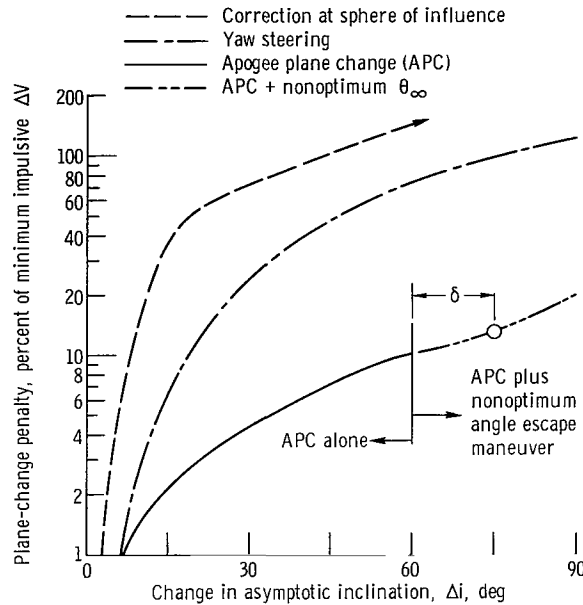


Figure 11. - Comparison of plane-change maneuvers; impulsive thrusts. Launch energy parameter $v_{\infty}^2 = 2$.

figure 11. Here, ΔV_{1wp} (expressed as a percentage of the minimum impulsive ΔV) is plotted against Δi for a relatively high-energy maneuver with $v_{\infty}^2 = 2$. The two upper curves apply to the one-burn escape maneuver and bound the possibilities available for that case (ref. 8). The dashed curve represents an auxiliary maneuver applied transversely near the sphere of influence. The dash-dotted curve denotes the use of yaw steering during the main maneuver; although this represents an improvement over the previous case, it is clear that both of them involve significant ΔV penalties for values of Δi greater than about 10° .

By comparison, the apogee-plane-change (APC) maneuver described by equations (12) is applicable to the two-burn escape mode. This yields penalties that are lower by one-half to one order of magnitude. As may be seen from the solid curve, this approach yields a penalty of 10 percent or less for values of Δi up to 60° .

Inclinations in the range $60^\circ < \Delta i \leq 90^\circ$ involve a pitch steering constraint (recall eq. (13)) in addition to the APC maneuver. That is, the difference δ between $\theta_{\infty, opt}$ and the right-hand side of equation (14) is made up by modifications of the second-burn power-on point $\nu_{o, 2}$ and the second-burn pitch program. Even when this is necessary, ΔV_{1wp} is reduced by a large factor. Thus, it may be concluded that the two-burn escape mode offers significant ΔV_{1wp} reductions, in addition to the initial mass and engine size advantages noted before.

Mission Applications

It has been shown that the two-burn escape mode offers attractive initial mass and engine size reductions over the entire spectrum of launch energies. The possible impact of this upon mission planning will now be illustrated by considering three specific mission examples.

Mars round trips. - A previous study of an ambitious manned Mars mission in the 1980 time period (ref. 9) indicates that total payloads⁴ injected on the Earth-Mars trajectory may approximate 500 000 kilograms for a trip time of 420 days. The corresponding launch energy parameter is $v_{\infty}^2 = 0.27$. Then, referring to figure 6(a) for mass-growth factors reveals that the two-burn escape mode leads to an initial mass savings of 60 000 kilograms out of 1.105×10^6 kilograms, or about 5.5 percent. Figure 7 shows that this savings is obtained for a time penalty of $\Delta T_m = 4.3$ hours.

Inspection of figure 8 now shows that $a_{o,1}$ is also reduced from 0.195 to 0.132 local gravities. Hence, the optimum thrust ratings are about 2.1×10^6 newtons for the single-burn maneuvers and about 1.3×10^6 newtons for two-burn maneuvers. This represents a reduction of nearly 40 percent in the desired thrust rating. The burning time is increased from 36 to 51 minutes.

Mars probes. - It was shown in the preceding section that the two-burn escape mode yields a conspicuous reduction of the desirable engine size and a smaller but still worthwhile initial mass saving when applied to a rather typical Mars round-trip mission using nuclear rockets. There are similar benefits in the case of a one-way probe mission using chemical rockets. For instance, single-stage chemical vehicle weighing 15 000 kilograms (33 000 lb) could inject a 5000-kilogram payload toward Mars (assuming the same outward transfer as previously) by using the two-burn mode, compared with 4690 kilograms with the one-burn mode. This improvement of 310 kilograms represents 5.3 percent more payload.

Jupiter probes. - As was previously seen in connection with figure 6, the two-burn mode yields progressively greater improvements for the higher launch energies. This technique is consequently of great interest for major planet missions which inherently require high launch energies.

A typical mission of this type was selected from the trajectory data presented in reference 4; the Earth-Jupiter trip time is 600 days and the launch energy parameter is $v_{\infty}^2 = 1.5$. Assuming a two-stage 15 000-kilogram vehicle, reference to figure 6(b) indi-

⁴This is based on "actual" payloads (i. e., crew and excursion modules and reentry systems) of about 70 000 kg with propulsive ΔV 's and upper stage parameters as in ref. 8.

cates that M_{pay} can be increased from 1818 to 2027 kilograms, an improvement of 11.5 percent.

In short, it has been illustrated that the present two-burn technique yields optimum nuclear engine size reductions of about 40 percent. The associated initial mass or payload improvements are appreciable even for low-energy missions and assume significant proportions at higher energies. These benefits are obtained at the cost of extending the mission time by a few hours or days and burn times by about 15 minutes; they also depend upon the availability of restartable engines.

Other Characteristics of Two-Burn Maneuvers

There are several other respects in which the two-burn escape mode may prove advantageous; these deserve passing mention even though they will not be discussed in detail.

Early abort capability. - It may be noted that the two-burn escape mode possesses an inherent early abort capability up through second-burn initiation. Any malfunction occurring at this point or before will leave the crew module in an elliptical geocentric orbit; thus rescue and salvage operations may be carried out promptly and with the full aid of the entire Earth-based tracking and communications network. In the case of two-stage vehicles, this capability may be extended through second-stage ignition with little penalty. It may be recalled from figure 5 ($M_{O,1}/M_{\text{pay}}$ plotted against $v_{\infty,sp}^2$) that the two-burn minimum is not only lower than that of the one-burn maneuver, but is also very flat. This means that the early abort capability (which requires $v_{\infty,sp}^2 < 0$) can be preserved through second-stage ignition with very little penalty if the two-burn approach is used. There is, by comparison, a conspicuous performance loss for doing this if one-burn maneuvers are used. Several two-stage vehicle maneuvers are shown in the last three rows of table II(d); by comparing these results with rows 2 to 4 it may be concluded that the early abort capability can be retained without major penalty except for extremely energetic maneuvers where $v_{\infty}^2 > 3$.

Reusable first stages. - The two-burn escape mode is by its nature compatible with a reusable first-stage vehicle configuration. That is, if the constraint $v_{\infty,sp}^2 < 0$ is imposed as previously, the spent first stage will in the natural course of events be left in a stable, highly eccentric geocentric orbit. Aftercooling propellant flow (which has been assumed to be entirely wasted up to this point) might then be used to produce either an atmospheric re-entry trajectory or another parking orbit. At this point, the stage could be refurbished, refueled, and reused. Alternatively, if a reusable first stage is used, it must necessarily be shut down at $v_{\infty,sp}^2 < 0$. In this case, the second stage might just as well coast on around the ellipse and take advantage of the favorable thrust-

ing region near periapse. Thus, it is seen that the two-burn escape mode and the recoverable first-stage vehicle configuration are closely related concepts. They complement one another nicely even though it is possible to have one without the other.

Additional tracking time. - It may be noted that the mission time penalty ΔT_m (see fig. 7) is all spent fairly close to the Earth. This extra time need not be entirely detrimental. With prolonged ground-based tracking, first-burn injection errors could possibly be identified during the coast and then corrected during the second burn. Further studies are indicated to determine whether the resulting overall guidance dispersions and, hence, midcourse ΔV requirements will be significantly affected by this approach.

CONCLUDING REMARKS

Earth-escape maneuvers involving two distinct burning periods separated by an intermediate, geocentric coasting ellipse have been studied herein. The first burn begins at an initial low circular parking orbit and terminates in the coasting ellipse. The second burn is initiated upon approaching the perigee of the coasting ellipse and terminates in the desired escape hyperbola.

When compared with the conventional single-burn type, the present maneuvers are shown to yield initial mass reductions ranging from about 5 percent at low energies to as much as 25 percent for high energy missions. They also lead to a decrease in optimum engine size of about 40 percent for burn times under 60 minutes, and (in the example shown) to as much as a 90 percent saving in the launch window ΔV penalty.

Side benefits of the present maneuvers include: (1) compatibility with reusable orbital launch vehicles, (2) enhanced abort, rescue, and salvage capabilities, and (3) possible improved utilization of available ground tracking and guidance facilities. These would at least partially offset the undesirable features; namely, greater complexity, need for restartable engines, slightly longer mission times, and extra Van Allen belt traversals.

Lewis Research Center,
National Aeronautics and Space Administration,
Cleveland, Ohio, September 26, 1968,
789-30-01-01-22.

1	first stage or first burn	♂	Mars
2	second stage or second burn	♃	Jupiter
∞	sphere of influence	♄	Saturn
☿	Mercury	♅	Uranus
♀	Venus	♆	Neptune
⊕	Earth		

REFERENCES

1. Johnson, Paul G. ; and Rom, Frank E. : Perigee Propulsion for Orbital Launch of Nuclear Rockets. NASA TR R-140, 1962.
2. Willis, Edward A. , Jr. : Finite-Thrust Escape and Capture Into Circular and Elliptic Orbits. NASA TN D-3606, 1966.
3. Anon. : Planetary Flight Handbook. Vol. 3 of Space Flight Handbooks. NASA SP-35, parts 1-3, 1963.
4. Luidens, Roger W. ; Miller, Brent A. : and Kappraff, Jay M. : Jupiter High-Thrust Round-Trip Trajectories. NASA TN D-3739, 1966.
5. Beck, Andrew J. ; and Divita, Edward L. : Evaluation of Space Radiation Doses Received Within a Typical Spacecraft. ARS J. , vol. 32, no. 11, Nov. 1962, pp. 1668-1676.
6. Powell, M. J. D. : An Efficient Method for Finding the Minimum of a Function of Several Variables Without Calculating Derivatives. The Computer J. , vol. 7, 1964, pp. 155-162.
7. Willis, Edward A. , Jr. : Optimal Finite-Thrust Transfer Between Planet Approach and Departure Asymptotes With a Specified Intermediate Orbit. NASA TN D-4534, 1968.
8. Deerwester, J. M. ; McLaughlin, J. F. ; and Wolfe, J. F. : Earth-Departure Plane Change and Launch Window Considerations for Interplanetary Missions. J. Spacecraft Rockets, vol. 3, no. 2, Feb. 1966, pp. 169-174.
9. Luidens, Roger W. ; Burley, Richard R. ; Eisenberg, Joseph D. ; Kappraff, Jay M. ; Miller, Brent A. ; Shovlin, Michael D. ; and Willis, Edward A. , Jr. : Manned Mars Landing Mission by Means of High-Thrust Rockets. NASA TN D-3181, 1966.

FIRST CLASS MAIL

05U 001 55 51 3DS 68013 00903
AIR FORCE WEAPONS LABORATORY/AFWL/
KIRTLAND AIR FORCE BASE, NEW MEXICO 8711

ATT E. LOU BOWMAN, ACTING CHIEF TECH. LI

POSTMASTER: If Undeliverable (Section 158
Postal Manual) Do Not Return

"The aeronautical and space activities of the United States shall be conducted so as to contribute . . . to the expansion of human knowledge of phenomena in the atmosphere and space. The Administration shall provide for the widest practicable and appropriate dissemination of information concerning its activities and the results thereof."

— NATIONAL AERONAUTICS AND SPACE ACT OF 1958

NASA SCIENTIFIC AND TECHNICAL PUBLICATIONS

TECHNICAL REPORTS: Scientific and technical information considered important, complete, and a lasting contribution to existing knowledge.

TECHNICAL NOTES: Information less broad in scope but nevertheless of importance as a contribution to existing knowledge.

TECHNICAL MEMORANDUMS: Information receiving limited distribution because of preliminary data, security classification, or other reasons.

CONTRACTOR REPORTS: Scientific and technical information generated under a NASA contract or grant and considered an important contribution to existing knowledge.

TECHNICAL TRANSLATIONS: Information published in a foreign language considered to merit NASA distribution in English.

SPECIAL PUBLICATIONS: Information derived from or of value to NASA activities. Publications include conference proceedings, monographs, data compilations, handbooks, sourcebooks, and special bibliographies.

TECHNOLOGY UTILIZATION PUBLICATIONS: Information on technology used by NASA that may be of particular interest in commercial and other non-aerospace applications. Publications include Tech Briefs, Technology Utilization Reports and Notes, and Technology Surveys.

Details on the availability of these publications may be obtained from:

SCIENTIFIC AND TECHNICAL INFORMATION DIVISION
NATIONAL AERONAUTICS AND SPACE ADMINISTRATION
Washington, D.C. 20546